

# Silicon nanostructures from electroless electrochemical etching

Kurt W. Kolasinski

*Department of Chemistry, University of Virginia, P.O. Box 400319, McCormick Road, Charlottesville, VA 22904-4319, United States*

## Abstract

Recent advances in the production of Si nanostructures from electroless etching are reviewed, including stain etching, metal-assisted etching and chemical vapour etching. A brief review of the explosion in applications of porous silicon over the past 18 months is also given. The stain film that results from the etching of (poly- or single-)crystalline Si is composed of a porous network of nanocrystalline silicon. Few mechanistic studies of electroless etching have been performed, but the more extensively studied anodic etching of silicon in fluoride solutions provides many clues as to how porous films are formed. Intriguing recent results have shown that control over the properties of the film can be obtained by exercising control over the composition of the etchant.

© 2006 Elsevier Ltd. All rights reserved.

*Keywords:* Stain etching; Porous silicon; Nanostructure; HF; Nanowire

## 1. Introduction

One of the great challenges of solid-state physics is to control the band structure of phonons and electrons to achieve desired properties: raising the  $T_c$  and critical current of superconductors, producing semiconductors with well-defined band gaps, increasing the efficiency of thermoelectric cooling, altering the catalytic activity of metals, etc. Surface science plays a fundamental role in addressing this challenge both in that it provides a means for understanding the underlying growth and etching phenomena [1] that affect the desired property and in that it provides a synthetic method for producing the materials that exhibit these properties. For example, surface texturing is used to align the grains of yttrium barium copper oxide (YBCO) in second-generation superconducting wires. CVD [2–4] and MBE [5–7] are used to engineer the band gaps of semiconducting multilayer structures [6,8–12] to produce an array of optoelectronic devices. Dispersing gold in nanoscale clusters across an oxide surface transforms this most noble of metals into one of the finest catalyst for CO oxidation [13].

In the world of nanotechnology, there are two grand schemes for making structures and devices: the top-down and the bottom-up approaches. In a slightly over-generalized form, we can define these two approaches thusly: The top-down approach rules the roost in the production of integrated circuits. It is the engineering approach that has led us to the amazingly successful world of \$4 billion fabs. In this world, perfection of individual processing steps is sought. One tries to keep the individual steps simple but the combination is very complicated. Hundreds of steps may be involved. No amount of processing complexity is too great as long as the process can be turned into a batch job that can be repeated millions of times at low cost. Making a layer consists of, for instance, taking a perfectly clean silicon wafer in a clean room environment, spin coating a polymer resist onto it, bringing an intricately designed mask into close proximity of the resist, exposing the resist with a short wavelength photon sources, chemically treated the exposed resist to remove either exposed or unexposed regions of resist, applying a material component to the pattern that has been created, removing unwanted material from regions outside of the pattern, rinse, lather, repeat for as many processing steps as are required. Even something as seemingly simple as “making a clean silicon surface” may take tens of processing steps.

*E-mail address:* [Kolasinski@virginia.edu](mailto:Kolasinski@virginia.edu)

In the bottom-up scenario, the processing steps are essentially infinitely complex but required little intervention on the scientist's part. The idea is to use chemistry to perform error checking and correcting processes that will guide themselves to the end product: the desired structure. The ideal is inspired by biomimetic processes: self assembly and self organization – the exploitation of non-covalent interactions to direct the formation of structures. It is in this realm that we are trying to create Si nanostructures by electroless etching. Just how far can we push chemistry with minimal process intervention to perform the tasks we want so that the process arrives at arbitrarily complex structures?

Specific to silicon, turning bulk Si into nanocrystals [14,15] or nanocrystalline networks [16,17] changes Si into a brilliant emitter in the visible because of the effects of quantum confinement. Hence there has been great interest in controlling and understanding the formation of nanocrystalline silicon [18]. We can understand how quantum confinement increases the band gap of a nanocrystalline semiconductor by analogy to the particle in the box problem. A smaller box leads to a greater spacing between energy levels, thus a larger band gap. Porous silicon (por-Si) is the most intensively studied variant of nanocrystalline silicon (nc-Si) and several reviews have been published regarding the formation [19–21], properties [17,22,23], surface chemistry [24], and photoluminescence (PL) [25–29] of por-Si. Amazing control over pore morphology has been demonstrated by Gösele and co-workers [30].

Electrochemical etching differentiates itself from chemical etching in that charge transfer is involved in the former. Hydroxide exhibits both chemical and electrochemical pathways, whereas etching in acidic fluoride is exclusively electrochemical [1]. Chemical etching of the type extensively studied, for instance, by Chabal and co-workers can be used to produce nearly perfectly flat and hydrogen-terminated Si surfaces [31–37].

There are four electrochemical routes to por-Si all of which occur in acidic fluoride solutions: anodic etching, photoelectrochemical etching, laser-assisted etching and electroless etching. The boundaries are not completely distinct and combined processes are known. Anodic etching involves the attachment of Si (the working electrode) and a counter electrode (usually Pt) to a power supply, which is used to regulate the voltage on the Si crystal. The electrochemistry that occurs is controlled by the voltage and solution composition. This works fine for p-type Si but for n-type Si, in addition to connecting the Si and counter electrode to the power supply, free carriers need to be made available by illumination of the Si electrode, hence the term photoelectrochemical etching. It is possible to dispense with the power supply and external counter electrode. By irradiating a small spot on a Si wafer, free carriers are produced and band bending is used to separate holes from electrons. In n-type Si, holes are forced to the surface of the irradiated area and por-Si forms there. In p-type Si, holes are forced to the unirradiated area and that is where

por-Si formation occurs [38]. Mechanistically, the chemical transformations that occur in these three types of etching are very much the same [39]. In electroless etching, electrochemistry occurs spontaneously without the intervention of a power supply or photon source. Three types of electroless etching are reviewed here: stain etching, metal-assisted etching and chemical vapour etching.

Stain etching is the etching that results from a solution composed of fluoride and an oxidant. In chemical vapour etching, the vapour of such a solution, rather than the solution itself is in contact with the Si. In metal-assisted etching deposited metal particles are also involved. Electroless etching of Si to form por-Si is a simple process that requires the attachment of no electrodes and can be performed on objects of arbitrary shape and size. Nonetheless, the formation of por-Si via electroless etching has received much less systematic investigation [17,40]. The preponderance of work has concentrated on use of HF in combination with a nitroxy oxidant, typically HNO<sub>3</sub> or NaNO<sub>2</sub>. It will be shown that this has severely limited the range of films and their properties and that the use of a wider range of fluoride carriers and oxidants can lead to greater control over morphology and properties.

## 2. Recent advances in porous silicon structures and devices

Within the past year, there has been a great proliferation of studies involving por-Si in device structures. Many of these advances are chronicled in the proceedings of the 4th International Conference on Porous Semiconductors – Science and Technology (PSST-2004), which was published in 2005 [41]. Specific areas in which por-Si is being implemented technologically include optoelectronics, sensors, mass spectrometry, nanocrystal production, drug delivery, biomaterials, fuel cells and photovoltaics.

Ever since Canham's observation of visible photoluminescence [16] there has been great interest in the possible application of por-Si in optoelectronics [42]. The implementation of por-Si in industrially relevant processes has proven to be challenging but progress continues towards the implementation of Si photonics [43] and theoretical understanding of the electronic states in nanocrystalline Si (nc-Si) continues to advance [44–46]. The proceedings of the 2004 Spring Meeting of the European Materials Research Society (E-MRS) titled "Si-based photonics: towards true monolithic integration" make for fascinating reading into the advances made in por-Si, nanocrystalline Si and Si multilayer structures for use in waveguides, photonic crystals, optical filters, reflectors, photodetectors, light emitting devices, sensors and even lab-on-chip applications. Tuneable photonic band gap materials can be made from por-Si that can be thermally or electrically modulated [47,48].

Linnros and co-workers [49,50] have made great strides in the fabrication of forests of free-standing Si quantum dot towers. They have observed [51] the photoluminescence from a single dot and found a linewidth as narrow as 2 meV at 35 K, proving the atomic like nature of the

emission from Si nanocrystals resulting from quantum confinement. The study of optical gain and stimulated emission in nanocrystalline Si continues to attract much attention [52–55]. Cloutier et al. [\*56] have reported threshold behaviour, optical gain, longitudinal cavity modes and linewidth narrowing, along with a collimated far-field pattern, all of which are indicative of amplification and stimulated emission at 1278 nm from Si patterned with an ordered array of nanopores. Yamamoto et al. [57] have reported Si-based all optical switch on the basis of circular polarization retention. The observation of ballistic electron transport by Koshida and co-workers [58,59] has led to the development of a solid-state light emitting device in which organic dyes are excited by ballistic electrons produced in por-Si. Doping Er and Yb into por-Si can produce a white light emitter [60]. By altering the layer structure of por-Si films, their optical birefringence can be tuned [61,62]. Zener tunnelling of light has been observed in optical superlattices composed of por-Si [63].

The application of por-Si to sensor technology appears to be particularly promising. An ammonia sensor based on por-Si [64] is now commercially available. The versatility of por-Si based sensors allows for structures to be made that can exhibit large enhancements in the sensitivity compared to, for example, conventional surface plasmon resonance devices [\*65]. Ultrasonic electron emission enables a three-dimensional (3D) image sensor [66]. A number of sensor applications have been reported in the past year: for organic solvents [67], an electrical [68] or interferometric [69] sensor for detection of DNA hybridization, a humidity sensor for respiration monitoring [70], a resistance based hydrogen sensor [71], an optical sensor for pesticides in solution [72], a biosensor for oligonucleotides based on capacitance measurements [73], a conductometric gas sensor with sub-ppm sensitivities [74], and a chemiluminescence detector for bacteria [75]. A number of different applications regarding biosensors have been reported [76–79]. By combining layers with different pore sizes, a device can be made that both separates biomolecules, e.g. sucrose and bovine serum albumin, and provides for detection via interferometric methods [\*80].

A recent advance in matrix assisted laser desorption/ionization (MALDI) is the use of por-Si substrates as the immobilization matrix [81,82]. This variant of MALDI is called desorption/ionization on porous silicon mass spectrometry (DIOS-MS) [83]. A dense forest of Si nanowires [84], tips [85] or a film with a column/void structure [70] may offer some advantages, particularly with application to proteomics.

Porous Si has also appeared in a number of energy related technologies. Porous silicon has been of growing interest to solar technology because of its potential to increase solar cell efficiency through reduced reflectivity and recombination losses, and expanded spectral response [86]. A particularly interesting development in this area is the construction of 3D p–n junction structure for betavoltaics and photovoltaics by Fauchet and co-workers [\*87]. The 3D structure exhibits an order of magnitude increase

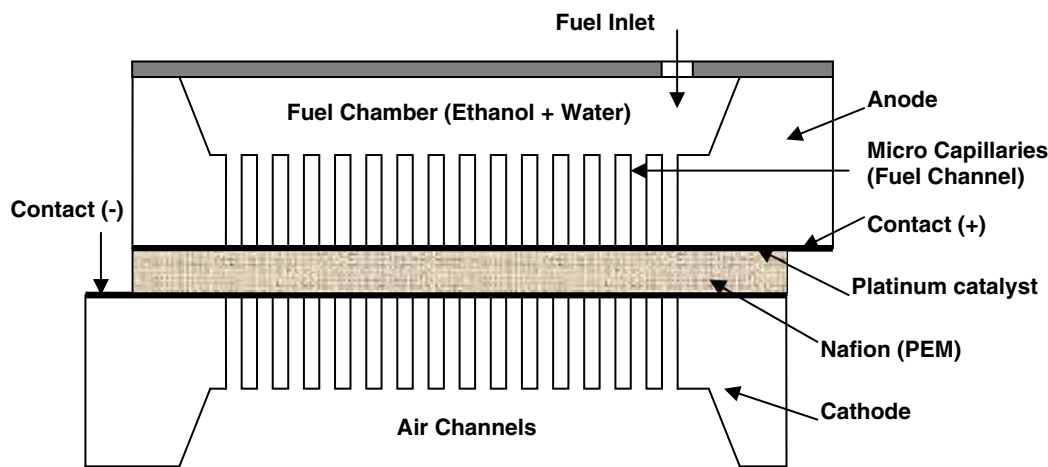
in efficiency compared to a planar structure. The geometry of these 3D porous diodes should provide significant enhancement in the performance of photodetectors and solar cells. Porous Si films have been investigated for anti-reflection coatings [88,89]. An antireflection coating of silicon nanowires formed by metal-assisted etching exhibits very low reflectivity but still has a lower efficiency than an uncoated photovoltaic cell, demonstrating that progress in improving carrier lifetimes must still be made [\*90]. Micropores formed by chlorine plasma etching rather than electrochemistry can also be used to lower the reflectivity of Si surfaces [91]. A sacrificial por-Si layer has been used to improve electrical performance in solar cells by gettering impurities [92–95]. CVD was used to deposit a 20- $\mu\text{m}$  thick c-Si layer on top of a free-standing por-Si film to produce a solar cell with 9.6% efficiency [96]. Another advance has been announced at IMEC [\*97]. A buried stack of alternating high (55%) and low (22.5%) porosity layers is used as a Bragg reflector to increase absorption in a thin epitaxial layer by reflecting light that has been transmitted in a first pass back into the epitaxial layer.

Nanostructured materials are of great interest for energy storage and conversion devices [98]. Porous Si has been investigated by Gole and co-workers [\*99] as an electrode for batteries. The production of miniature fuel cells using a Si substrate presents the advantages of serial and parallel integration. Micro-fuel cells have been built with a por-Si layer supporting an electrode and providing channels for fuel flow [100], including a direct ethanol fuel cell [101], which is depicted in Fig. 1. Pichonat and Gauthier–Manuel [\*102] have developed a proton-conducting membrane consisting of por-Si onto which molecules with acid groups are grafted. The membranes can be optimized not only by adjusting the characteristics of the por-Si film (pore size and structure) but also by changing the nature of the grafted molecules.

Biological applications of porous silicon relate not only to sensing but also to drug delivery, studies of cell/surface interactions and biomaterials. Por-Si is particularly interesting in a biological context because it is both biocompatible [103] and bioresorbable [104,105]. The incorporation of Si into hydroxyapatite has been studied in the context of developing artificial bone [106] because it enhances its biocompatibility. Sailor's group [107] has probed how the surface chemistry and pore structure can be optimized both for the uptake and the release of the steroid dexamethasone. Salonen and co-workers have investigated carbonized mesoporous Si particles for oral dosing of drugs [108,109]. Fonash and co-workers [70] have shown promoted attachment, differentiation, and proliferation of prokaryotic and eukaryotic cells on por-Si with a column/void structure as well as preferential adhesion of FL83B hepatocytes to por-Si relative to borosilicate glass.

### 3. Stain etching

Robins and Schwartz [110–112] and Turner [\*113] were among the first to study systematically the etching of Si in



© Elsevier 2004

Fig. 1. Cross-sectional view of the porous silicon based micro-direct ethanol fuel cell (DEFC) stack. The macroporous Si layer provides channels for contact of air and fuel with the electrodes. Reprinted with permission from S. Aravamudhan, A. R. A. Rahman, S. Bhansali, *Sens. Actuators A* 2005, 123–124, 497.

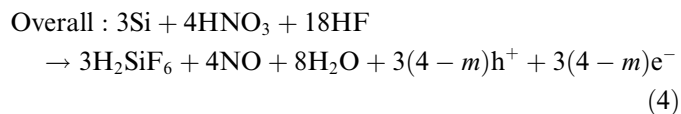
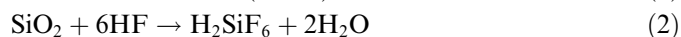
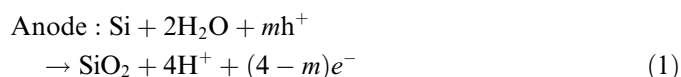
fluoride plus oxidant solutions. Robins and Schwartz concentrated on the electropolishing regime in which the silicon is etched isotropically leaving a more or less smooth surface and no porous film. Turner was the first to study stain etching in which a por-Si film is produced. This followed the discovery of por-Si formation via an electrochemical route by the Uhlirs [114]. Some time elapsed before it was realized that por-Si films produced either electrochemically [16] or by stain etching [115,116] can produce luminescent por-Si films as long as crystalline or polycrystalline substrates are used. Visible luminescence is not observed when amorphous Si is stain etched [117].

Turner [\*113] proposed that stain etching is actually electrochemical in its action, that is, there are anodic and cathodic sites on the surface of the semiconductor with local cell currents flowing between them. This assertion is supported by structural studies, such as those of Beale et al. [118] and Schoisswohl et al. [119], in which it was reported that the structure of anodically and stain etched por-Si is similar and, therefore, their formation mechanisms must share much in common. Si goes into solution at the anodic sites while the oxidant is reduced at the cathodic areas. If the etching process is non-preferential and material is removed uniformly, any given area on the surface continually alternates between being anodic and cathodic. When one spot is anodic much more than it is cathodic an etch pit will form. Conversely, hillocks are formed on areas that are cathodic more than they are anodic. From such anisotropy, pores develop.

Semiconductor etching occurs by oxidation of the semiconductor followed by removal of surface atoms. However, oxidation is a chemically ambiguous word and this has led to some mechanistic confusion. Often etching is said to occur by the formation of an oxide followed by chemical dissolution of the oxide layer. This is true of Si etching in the electropolishing regime, (+0.7 V with respect to the normal hydrogen electrode [120]), where an oxide grows, it is removed by HF(aq) via chemical etching [121–123]

and no por-Si is formed. But is this true in the por-Si formation regime? Alternatively, for por-Si to form, is the relevant oxidation step the increase in the Si oxidation state to a more positive value without the formation of an oxide?

It is now known that por-Si formation whether initiated electrochemically, photoelectrochemically or by laser irradiation, is initiated by the formation of valence band holes at the silicon surface. A number of models have been proposed to explain etching in these regimes including those of Kooij and Vanmaekelburgh [\*124]; Gerischer, and coworkers [\*125,126]; Kang and Jorné [127]; Lehmann and Gösele [\*128]; and Kolasinski [\*39]. Turner proposed the following reactions for etchants composed of HNO<sub>3</sub>, HF and H<sub>2</sub>O:



These are composite reactions rather than elementary steps. What is clear from studies to elucidate the elementary steps in (photo)electrochemical etching [38,\*125,129] is that the fluoride species which control the kinetics of etching are HF and HF<sub>2</sub><sup>-</sup>.

As Eq. (1) shows, hole production in the valence band is again a crucial step in the initiation of the etching reaction. Here, *n* is the average number of holes required to dissociate one Si atom. Since Turner's time this chemical scheme has been accepted almost without further comment, even though no clear evidence has been presented that SiO<sub>2</sub> is formed as an intermediate [130] and one must ask why the formation of por-Si from stain etching is so much different from the common mechanism that describes anodic,

photoelectrochemical and laser-assisted etching in fluoride solutions. In Turner's reaction scheme, NO is the only gas evolved. It has been suggested [131] that NO<sup>+</sup> is the active nitrogen species or that NO<sub>2</sub><sup>-</sup> catalyzes the reaction [40].

The role and rate of oxide formation must be crucial to por-Si formation. SiO<sub>2</sub> is etched rapidly and isotropically by acidic fluoride solutions [132–134]. If a uniform film of SiO<sub>2</sub> results from the interaction of the oxidant with the surface, then this film will be removed *uniformly* by the action of the fluoride component. Electropolishing rather than por-Si formation ensues. If SiO<sub>2</sub> is formed during por-Si formation it is crucial, therefore, that the SiO<sub>2</sub> be formed heterogeneously on the surface. In effect, it must only form at the bottom of pits such that these pits develop into pores. Its formation on sidewalls and hillocks must somehow be suppressed to avoid the isotropic etching of pores that would lead to their removal. If SiO<sub>2</sub> formation is important in stain etching, then the role of the oxidant is to somehow facilitate the formation of an inhomogeneous oxide layer. One necessary condition for the formation of this layer is that the rate of oxidation must not exceed the capacity of the fluoride solution to etch the oxide; otherwise, the oxide coverage will grow until it covers the surface and isotropic etching will result.

It seems unlikely that a surface oxide plays a significant role in por-Si formation and this idea is further bolstered by examining etching in alkaline solutions [1]. Etching with hydroxide does not lead to por-Si formation. Porous Si forms in a fluoride solution because the etching reaction is self-limiting, whereas etching with OH<sup>-</sup> is not similarly constrained. Consider the models of Lehmann and Gösele [\*128] and Frohnhoff et al. [135]. Si etching in acidic fluoride solutions is an electrochemical process and responds to the electronic structure of the Si. Quantum confinement effects widen the band gap when Si nanostructures drop below ~5 nm in size [136]. The walls of the pores then become effectively passivated because there is a depletion of holes within the confined structures and holes are required to initiate the etching sequence. Holes are instead directed to the bottoms of pores, which are connected to unconfined bulk Si and etching proceeds there. Hydroxide does not experience a similar quantum confinement related constraint because it can etch via a chemical pathway. Porous Si is not stable in OH<sup>-</sup>(aq) and is quite efficiently removed by it. In the absence of a self-limiting constraint on oxide formation and since the chemical dissolution of oxide by HF(aq) is isotropic, there is no driving force to instigate the formation of quantum-confined structures as the result of oxide formation.

Consequently, the way to look at the role of the oxidant is to think of it purely as an electrochemical oxidant rather than a producer of silicon oxides. Considering Eq. (3) we see that the crucial role of the oxidant is to inject holes into the valence band. In this manner the oxidant, or more precisely its electrochemical potential, takes on the role of either the voltage in electrochemical etching or the photon energy in laser-assisted etching. Therefore, crucial proper-

ties of the oxidant will be its electrochemical potential and the rate at which it can transfer charge with the Si surface. In order to inject holes into the valence band, an electron acceptor level of the oxidant must lie at or below the valence band maximum (VBM), as shown in Fig. 2. Hence, the electrochemical potential of the oxidant must be sufficiently positive. Furthermore, by identifying the role of the oxidant in initiating etching and the importance of quantum confinement to create self-limiting charge injection, we can now identify the electrochemical potential of the oxidant as a control parameter that can be used to influence por-Si formation.

Kolasinski [\*39] has shown that the hole is injected into a bulk band and that hole injection directly into the Si–H bond is energetically impossible under the conditions of most electrochemical, photoelectrochemical, laser-assisted etching or stain etching experiments. Thus models of stain etching involving hole injection into the Si–H bond [137] are not feasible. The presence of a valence band hole changes the effective sticking coefficient of F<sup>-</sup>(aq) from  $\leq 5 \times 10^{-11}$  to ~1. Hole injection is the switch that turns on Si etching activity in acidic fluoride solutions whereas OH<sup>-</sup> is the initiator of reactivity in solutions near and above neutral pH [\*39].

Nahidi and Kolasinski [\*\*138] have used an understanding of how stain etching is initiated to control the photoluminescence spectrum and by implication the nanocrystallite size distribution. They used oxidants with different electrochemical potentials  $E_0$  (Fe(III), HNO<sub>3</sub>, MnO<sub>4</sub><sup>2-</sup>) and found that the PL peak wavelength correlates with  $E_0$ : a more positive value of  $E_0$  leads to bluer PL as shown in Fig. 3.

Furthermore, consistent with the controlling role of the oxidant on the basis of its role in hole injection into the valence band according to (e.g. for Fe(III) as oxidant)

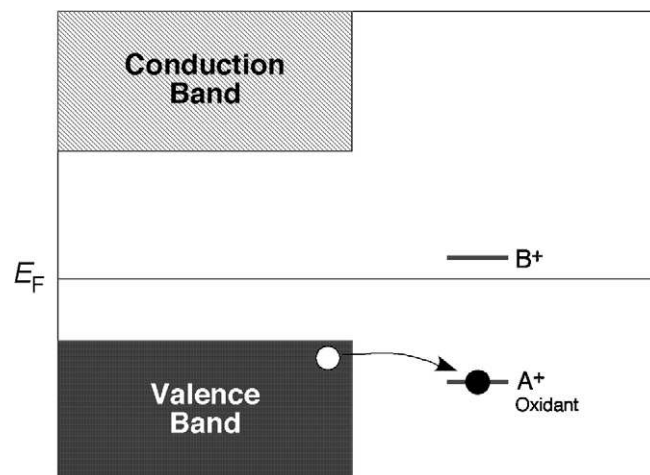
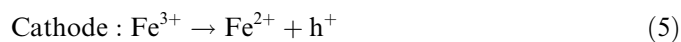


Fig. 2. Hole injection can occur via an acceptor level such as A<sup>+</sup>, that lies below the VBM but not one such as B<sup>+</sup> that lies above it.

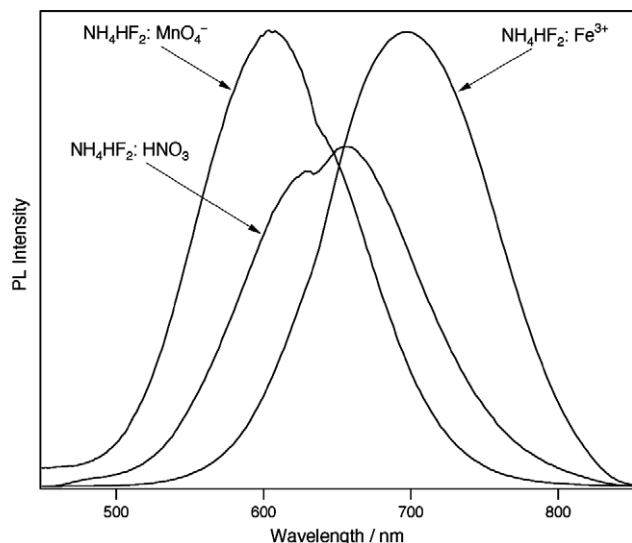
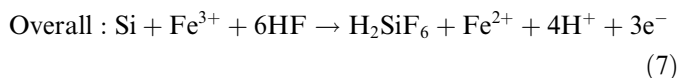


Fig. 3. The PL from films etched with  $\text{Fe}^{3+}$  ( $E_0 = 0.47$  V versus the standard calomel electrode (SCE)) peaks at 696 nm, compared to 654 nm for  $\text{HNO}_3$  ( $E_0 = 0.66$  V) and 604 nm for  $\text{MnO}_4^-$  ( $E_0 = 1.19$  V).

they have shown [138] that stain etching can proceed with minimal bubble formation and without the need to invoke surface oxide formation.



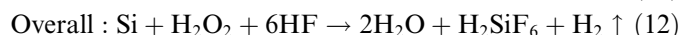
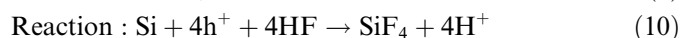
#### 4. Metal-assisted etching

Dimova-Malinovska et al. [139] demonstrated stain etching in the presence of an evaporated Al layer can produce luminescent por-Si. Kelly and co-workers [140,141] investigated the electrochemistry of Galvanic cell formation when a noble metal is short circuited to Si in the presence of an oxidant and demonstrated that the formation of microporous Si is possible in aerated HF and that macroporous Si can be produced in 5% HF + 1%  $\text{H}_2\text{O}_2$  in combination with pre-patterning of the surface with inverted pyramids. Metal-assisted electroless etching to form por-Si was developed further by Bohn and co-workers [142–145] who significantly improved the process by using thinner films. Au, Pt or Au/Pt films ( $3 \text{ nm} \leq h \leq 20 \text{ nm}$ ) were deposited on a Si substrate. Etching was carried out in an HF/ $\text{H}_2\text{O}_2$ / $\text{CH}_3\text{OH}$  (or  $\text{CH}_3\text{CH}_2\text{OH}$ ) solution. Depending on the type of metal deposited and Si doping type and doping level, por-Si films with different morphologies and light-emitting properties were produced on the time scale of seconds in the dark or under ambient lights, on both p- and n-type Si.

By patterning the Pt deposit, the resulting porous film can also be patterned. Chattopadhyay and Bohn [145] have used a  $\text{Ga}^+$  focused ion beam to dissociate an organometallic precursor and deposit Pt in squares with 1.25–20  $\mu\text{m}$  edges. The squares are composed of a mixture of C, Si,

O, Pt and Ga. Etching occurs under and close to the deposits and results in a highly non-uniform film. Alternatively [143], the Si substrate can be covered with an octadecyltrichlorosilane (OTS) monolayer patterned using micro-contact printing. Pt is deposited in areas not covered with OTS and por-Si that luminescence around 580 nm upon UV illumination is formed in the Pt-coated regions.

Thin metal coatings facilitate the etching in HF and  $\text{H}_2\text{O}_2$ , and of the metals investigated, Pt yields the fastest etch rates and produces por-Si with the most intense PL. Gas evolution from the metal-coated area was clearly observed, especially for Pt and Au/Pd. For these metals no metal dissolution was observed, in contrast to the behaviour using Al. Li et al. [142] proposed a reaction scheme involving local coupling of redox reactions with the metal to explain the metal-assisted etching process.



Hole injection in this case is provided by the reaction of  $\text{H}_2\text{O}_2$  on the metal particle. The holes are injected into the Si valence band and then diffuse away from the metal particle explaining why etching is confined to the near-particle area. Dissolved  $\text{O}_2$  can also play the role of oxidant but leads to etching at a very low rate [146].

Gorostiza and co-workers [147–149] have studied the deposition of Pt and Ni in fluoride solutions onto Si with regard to charge exchange and por-Si formation. In the absence of metal ions, the Fermi level of n- and p-type Si lies close to  $E^0(\text{H}^+/\text{H}_2)$  at the open circuit potential (OCP) as depicted in Fig. 4. This steady-state equilibrium can be described as a dynamic equilibrium between two opposite reactions: the anodic one being the dissolution of the substrate and the other being the reduction of pro-

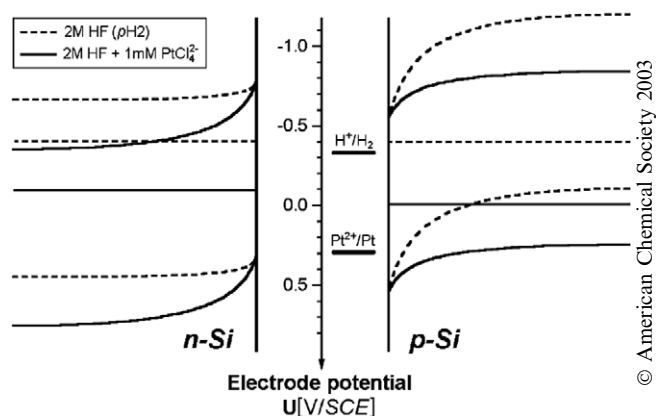


Fig. 4. Experimental energy diagram of the interface between Si and a blank fluoride solution (---) at pH 2 and fluoride solution (—) in the presence of 1 mM  $\text{Pt}^{2+}/\text{Pt}$ . Reprinted with permission from P. Gorostiza, P. Allongue, R. Diaz, J.R. Morante, F. Sanz, J. Phys. Chem. B 2003, 107, 6454.

tons ( $\text{H}_2$  evolution) and dissolved oxygen. Luminescent por-Si is formed during Pt deposition. No bubbles are formed during por-Si formation. They infer that the  $\text{H}_2$  formed from the etch products' reaction with water is reoxidized to protons. The electrons produced have energies close to the Fermi level of Pt clusters. They may either be re-emitted from the Pt clusters into the Si or recombine with holes. The latter process is more likely, with the interface states at the Pt/Si contacts acting as recombination centres. Ni deposits autocatalytically on Si from fluoride solutions of pH 8, because the  $\text{Ni}/\text{Ni}^{2+}$  level lies within the Si band gap. Deposition is accompanied by visible  $\text{H}_2$  evolution and no por-Si formation. No Ni deposition or hydrogen evolution is observed at low pH.

A number of studies have appeared in the past year involving electroless metal-particle-assisted etching [150,151]. Peng and co-workers (see Fig. 5) have used etching in  $\text{HF}/\text{AgNO}_3$  solutions to form films composed of aligned Si nanowires (SiNW) [\*90,152–\*\*155]. Etching displays little crystallographic dependence and can be performed on crystalline or polycrystalline substrates. Etching for 20 min at  $50^\circ\text{C}$  creates a film approximately  $10\ \mu\text{m}$  thick. After etching Ag particles remain in the film. The films exhibit very low reflectivity, which makes them attractive for solar cell applications [\*90]. Ag nanoparticles deposit out of solution onto the surface of the substrate. They catalyze the etching reaction, sink below the surface and leave behind columns of Si nanostructures. If only  $\text{AgNO}_3$  is used, then Ag dendrite formation accompanies SiNW formation. These can be avoided by the replacing  $\text{AgNO}_3$  after a short period with  $\text{Fe}(\text{NO}_3)_3$ .

$\text{HF}/\text{H}_2\text{O}_2$  mixtures have been used by Tsujino and Matsumura [156,157] to etch cylindrical and helical pores in c-Si. Ag, Pt, Pd or Cu particles are deposited by electroless plating and then exposed to the solution. The top of the wafer is covered by an up to  $3\ \mu\text{m}$  thick microporous layer

when etched in a 10:1 (v:v) solution of 10% HF and 30%  $\text{H}_2\text{O}_2$  and with Pt as the deposited metal. This layer exhibits visible PL. The microporous layer is only 300 nm thick when Ag is used. What most strikingly differentiates Ag from other Pd and Cu is that straight macropores on Si(100) or inclined macropores on Si(111) exist below the microporous region. Sometimes for Pt, cylindrical or helical pores are found below the microporous region. The helical macropores are also sometimes observed for Ag. Switching from cylindrical to helical pores is accomplished by changing the solution concentrations and the walls of the macropores are lined with microporous silicon. Ag particles are found at the bottoms of these macropores, with a diameter matching that of the pore. If the etching time is extended to 10 h, pores as deep as  $500\ \mu\text{m}$  and  $\sim 50\ \text{nm}$  in diameter are found.

Cruz et al. [158] have studied  $\text{HF}/\text{H}_2\text{O}_2/\text{CH}_3\text{CH}_2\text{OH}$  etching with Au or Pt particles and found that the etch depth and film morphology respond to doping level but not doping type. The metal films ( $1\ \text{nm} \leq h \leq 8\ \text{nm}$ ) were deposited by vacuum sputtering. Pore morphology also depends on the metal. Au is found to form a more columnar structure at a higher rate as opposed to a spongy structure for Pt. They did observe the formation of some straight macropores but always in the presence of interconnecting lateral pores. Etch depth was proportional to etch time up to 3 h at which point it stopped. Increased temperature ( $40^\circ\text{C}$  versus room temperature) increases the etch rate.

## 5. Chemical vapour etching

An interesting but not well understood variation on stain etching is that of chemical vapour etching (CVE) [159–163]. In CVE a solution is made up from concentrated HF plus concentrated  $\text{HNO}_3$ . However, instead of dipping the Si substrate in the solution, the substrate is held above the solution and the temperatures of the solution, the substrate and the time of exposure are controlled. Depending on these parameters, either a por-Si layer or a layer composed primarily of  $(\text{NH}_4)_2\text{SiF}_6$  with a thin por-Si transition layer is formed. Both layers are photoluminescent. Koker et al. [164] have demonstrated that the luminescence associated with a hexafluorosilicate/por-Si interface is blue-shifted compared to the PL from the pure por-Si layer. A similar trend was found by Saadoun et al. [162]. As ammonium hexafluorosilicate is water soluble and por-Si is soluble in alkaline solutions, CVE can be used to form grooves in Si, which is of interest for the use of por-Si in solar cell technology [94,95,159,160].

The mechanism of etching in this regime is not well understood. Infrared spectroscopy reveals a combination of hydrogen termination and oxidation of the surface [159,161,162]. When too much condensation occurs and droplets form on the surface, por-Si formation is suppressed [163]. Capillary condensation in the pores may be occurring before droplets are observed on the external surface. If Eq. (2) were the only way to remove Si from the

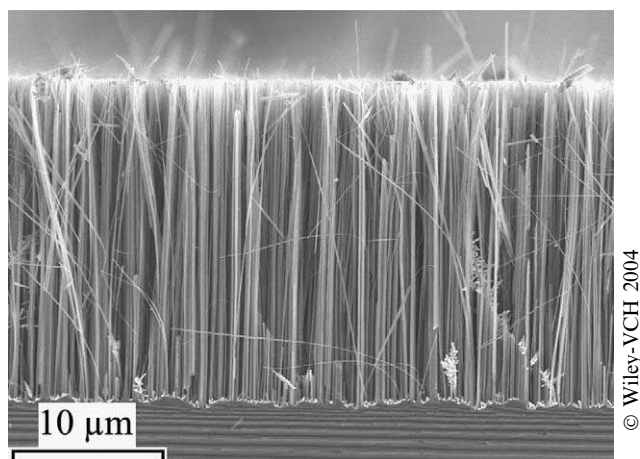


Fig. 5. A cross-sectional electron micrograph of a por-Si film composed of vertical Si nanowires. The film was created by etching in a  $4.6\ \text{mol dm}^{-3}$   $\text{HF} + 0.02\ \text{mol dm}^{-3}$   $\text{AgNO}_3$  solution for 60 min at  $50^\circ\text{C}$ . Reprinted with permission from K. Q. Peng, Z. P. Huang, J. Zhu, *Adv. Mater.* 2004, 16, 73.

surface, then there would be no way to etch Si in the absence of hexafluorosilicate formation. However, the initial etch product [1,\*39] is a volatile compound such as  $\text{HSiF}_3$  and this primary product hydrolyzes to the hexafluorosilicate. If the hydrolysis reaction is slow, the volatile primary etch product can be lost to the gas phase before forming a product that can precipitate on the surface.

## 6. Conclusions and perspectives

Over the last two years there has been an explosion in the applications of porous silicon to a variety of technological areas including sensors, energy, biomedical technology, optoelectronics and analytical chemistry. Progress in these areas appears to be accelerating. Anodic etching of silicon remains the most intensively studied and most controllable synthetic method for por-Si production, particularly in that it can be used to produce multilayer stacks of different porosity or combined with lithographic positioning of pore nucleation to create macroporous silicon. Nonetheless, electroless etching because of its simplicity and ability to etch arbitrarily shaped objects such as Si pillars [165,166] offers some advantages. There is still much to learn about the mechanisms involved in electroless etching, particularly for metal-assisted etching. Can morphological control be further enhanced? The films produced by metal-assisted etching present a much different structure than conventional por-Si. Some of the stain etched films show evidence for superstructures imposed on combinations of micro- and macroporous silicon. Greater mechanistic understanding in the future should lead to greater control over the structure and properties of the films produced.

## Acknowledgements

It is with pleasure that I acknowledge a critical reading of this manuscript by Joseph Maurer and Giovanni Zangari. I also thank Shyam Aravamudhan and Shekhar Bhansali for providing Fig. 1, Fausto Sanz for providing Fig. 4, and Kuiqing Peng and Jing Zhu for providing Fig. 5. This work was supported by the University of Virginia and the National Science Foundation IGERT Program under Grant # 9972790.

## References

The papers of particular interest have been highlighted as:

\* of special interest;

\*\* of very special interest.

- [1] Kolasinski KW. Growth and etching of semiconductors. In: Hasselbrink S, Lundqvist I, editors. Handbook of surface science, vol. 3. Amsterdam: Elsevier; in press.
- [2] Mooney PM. Strain relaxation and dislocations in SiGe/Si structures. Mater Sci Eng, R 1996;17:105.
- [3] Paul DJ. Si/SiGe heterostructures: from material and physics to devices and circuits. Semicond Sci Technol 2004;19:R75.
- [4] Rosei F. Nanostructured surfaces: challenges and frontiers in nanotechnology. J Phys: Cond Matter 2004;16:S1373.
- [5] Nishinaga T. Atomistic aspects of molecular beam epitaxy. Prog Cryst Growth Charact Mater 2004;48/49:104.
- [6] Franchi S, Trevisi G, Seravalli L, Frigeri P. Quantum dot nanostructures and molecular beam epitaxy. Prog Cryst Growth Characterization Mater 2003;47:166.
- [7] Joyce BA, Vvedensky DD. Self-organized growth on GaAs surfaces. Mater Sci Eng, R 2004;46:127.
- [8] Howe P, Abbey B, Le Ru EC, Murray R, Jones TS. Strain-interactions between InAs/GaAs quantum dot layers. Thin Solid Films 2004;464–465:225.
- [9] Le Ru EC, Howe P, Jones TS, Murray R. Strain-engineered InAs/GaAs quantum dots for long-wavelength emission. Phys Rev B 2003;67:165303.
- [10] Xie Q, Madhukar A, Chen P, Kobayashi NP. Vertically self-organized InAs quantum box islands on GaAs(100). Phys Rev Lett 1995;75:2542.
- [11] Mi Z, Bhattacharya P. Molecular-beam epitaxial growth and characteristics of highly uniform InAs/GaAs quantum dot layers. J Appl Phys 2005;98:023510.
- [12] Priester C, Lannoo M. Growth aspects of quantum dots. Curr Opin Solid State Mater Sci 1997;2:716.
- [13] Chen MS, Goodman DW. The structure of catalytically active gold on titania. Science 2004;306:252.
- [14] Wilcoxon JP, Samara GA. Tailorable, visible light emission from silicon nanocrystals. Appl Phys Lett 1999;74:3164.
- [15] Akcakir O, Therrien J, Belomoin G, Barry N, Muller JD, Gratton E, et al. Detection of luminescent single ultrasmall silicon nanoparticles using fluctuation correlation spectroscopy. Appl Phys Lett 2000;76:1857.
- [16] Canham LT. Silicon quantum wire array fabrication by electrochemical and chemical dissolution of wafers. Appl Phys Lett 1990;57:1046.
- [17] Cullis AG, Canham LT, Calcott PDJ. The structural and luminescence properties of porous silicon. J Appl Phys 1997;82: 909.
- [18] Kolasinski KW. Laser-assisted restructuring of silicon over nano-, meso- and macro-scales. In: Pandalai SG, editor. Recent research advances in applied physics, vol. 7. Kerala, India: Transworld Research Network; 2004. p. 267.
- [19] Föll H, Christophersen M, Carstensen J, Hasse G. Formation and application of porous silicon. Mater Sci Eng, R 2002;39:93.
- [20] Lehmann V. Electrochemistry of silicon: instrumentation, science, materials and applications. Weinheim: Wiley-VCH; 2002.
- [21] Zhang XG. Morphology and formation mechanisms of porous silicon. J Electrochem Soc 2004;151:C69.
- [22] Canham L. Properties of porous silicon. London: Institution of Electrical Engineers; 1997.
- [23] Koshida N, Matsumoto N. Fabrication and quantum properties of nanostructured silicon. Mater Sci Eng, R 2003;40:169.
- [24] Sailor MJ, Lee EJ. Surface chemistry of luminescent silicon nanocrystallites. Adv Mater 1997;9:783.
- [25] Bisi O, Ossicini S, Pavesi L. Porous silicon: A quantum sponge structure for silicon based optoelectronics. Surf Sci Rep 2000;38:1.
- [26] Lockwood DJ. Optical properties of porous silicon. Solid State Commun 1994;92:101.
- [27] John GC, Singh VA. Porous silicon: theoretical studies. Phys Rep 1995;263:93.
- [28] Kanemitsu Y. Light emission from porous silicon and related materials. Phys Rep 1995;263:1.
- [29] Fauchet PM. Photoluminescence and electroluminescence from porous silicon. J Lumin 1996;70:294.
- [30] Matthias S, Müller F, Schilling J, Gösele U. Pushing the limits of macroporous silicon etching. Appl Phys A 2005;80:1391.
- [31] Burrows VA, Chabal YJ, Higashi GS, Raghavachari K, Christman SB. Infrared spectroscopy of Si(111) surfaces after HF treatment: hydrogen termination and surface morphology. Appl Phys Lett 1988;53:998.

- [32] Chabal YJ, Higashi GS, Raghavachari K, Burrows VA. Infrared spectroscopy of Si(111) and Si(100) surface after HF treatment: Hydrogen termination and surface morphology. *J Vac Sci Technol, A* 1989;7:2104.
- [33] Higashi GS, Chabal YJ, Trucks GW, Raghavachari K. Ideal hydrogen termination of the Si(111) surface. *Appl Phys Lett* 1990;56:656.
- [34] Trucks GW, Raghavachari K, Higashi GS, Chabal YJ. Mechanism of HF etching of silicon surfaces: a theoretical understanding of hydrogen passivation. *Phys Rev Lett* 1990;65:504.
- [35] Trucks GW, Raghavachari K, Higashi GS, Chabal YJ. Trucks et al. reply. *Phys Rev Lett* 1991;66:1648.
- [36] Jakob P, Chabal YJ, Raghavachari K, Becker RS, Becker AJ. Kinetic model of the chemical etching of Si(111) surfaces by buffered HF solutions. *Surf Sci* 1992;275:407.
- [37] Chabal YJ, Harris AL, Raghavachari K, Tully JC. Infrared spectroscopy of H-terminated silicon surfaces. *Int J Mod Phys B* 1993;7:1031.
- [38] Koker L, Kolasinski KW. Investigations of the photoelectrochemical etching of Si and porous Si in aqueous HF. *Phys Chem Chem Phys* 2000;2:277.
- [\*39] Kolasinski KW. The mechanism of Si etching in fluoride solutions. *Phys Chem Chem Phys* 2003;5:1270.
- [40] Jones LA, Taylor GM, Wei F-X, Thomas DF. Chemical etching of silicon: Smooth, rough and glowing surfaces. *Prog Surf Sci* 1995;50:283.
- [41] *Phys Stat Sol A* 2005;202:1347–718.
- [42] Lockwood DJ, Pavesi L. Silicon fundamentals for photonics applications. In: Lockwood DJ, Pavesi L, editors. *Silicon photonics*, vol. 94. Berlin: Springer-Verlag; 2004. p. 1–50.
- [43] *Opt. Mater.* 2005;27:731–1109.
- [44] Zhao X, Wei CM, Yang L, Chou MY. Quantum confinement and electronic properties of silicon nanowires. *Phys Rev Lett* 2004; 92:236805.
- [45] Sundholm D. Density functional studies of the luminescence of Si<sub>29</sub>H<sub>36</sub>. *Phys Chem Chem Phys* 2004;6:2044.
- [46] Lehtonen O, Sundholm D. Density-functional studies of excited state of silicon nanoclusters. *Phys Rev B* 2005;72:085424.
- [47] Weiss SM, Haurylau M, Fauchet PM. Tunable photonic band-gap structures for optical interconnects. *Opt Mater* 2005;27:740.
- [48] Weiss SM, Ouyang HM, Zhang JD, Fauchet PM. Electrical and thermal modulation of silicon photonic bandgap microcavities containing liquid crystals. *Opt Express* 2005;13:1090.
- [49] Juhasz R, Elfström N, Linnros J. Controlled fabrication of silicon nanowires by electron beam lithography and electrochemical size reduction. *Nano Lett* 2005;5:275.
- [50] Kleimann P, Badel X, Linnros J. Toward the formation of three-dimensional nanostructures by electrochemical etching of silicon. *Appl Phys Lett* 2005;86:183108.
- [\*\*51] Sychugov I, Juhasz R, Valenta J, Linnros J. Narrow luminescence linewidth of a silicon quantum dot. *Phys Rev Lett* 2005;94: 087405.
- [52] Cazzanelli M, Kovalev D, Dal Negro L, Gaburro Z, Pavesi L. Polarized optical gain and polarization-narrowing of heavily oxidized porous silicon. *Phys Rev Lett* 2004;93:207402.
- [53] Fauchet PM, Ruan J, Chen H, Pavesi L, Dal Negro L, Cazzanelli M, et al. Optical gain in different silicon nanocrystal systems. *Opt Mater* 2005;27:745.
- [54] Ruan J, Fauchet PM, Dal Negro L, Cazzanelli M, Pavesi L. Stimulated emission in nanocrystalline silicon superlattices. *Appl Phys Lett* 2003;83:5479.
- [55] Luterova K, Cazzanelli M, Likforman JP, Navarro D, Valenta J, Ostatnicky T, et al. Optical gain in nanocrystalline silicon: comparison of planar waveguide geometry with a non-waveguiding ensemble of nanocrystals. *Opt Mater* 2005;27:750.
- [\*56] Cloutier SG, Kossyrev PA, Xu J. Optical gain and stimulated emission in periodic nanopatterned crystalline silicon. *Nature Mater* 2005;4:887–91.
- [57] Yamamoto N, Matsuno T, Takai H, Ohtani N. Circular polarization control in silicon-based all-optical switch. *Jpn J Appl Phys* 2005;44:4749.
- [58] Kojima A, Koshida N. Ballistic transport mode detected by picosecond time-of-flight measurements for nanocrystalline porous silicon layer. *Appl Phys Lett* 2005;86.
- [59] Nakajima Y, Uchida T, Toyama H, Kojima A, Gelloz B, Koshida N. A solid-state multicolor light-emitting device based on ballistic electron excitation. *Jpn J Appl Phys, Part 1* 2004;43:2076.
- [60] Luo L, Zhang XX, Li KF, Cheah KW, Shi HX, Wong WK, et al. Form birefringence of anisotropically nanostructured silicon. *Adv Mater* 2004;16:1664.
- [61] Kunzner N, Diener J, Gross E, Kovalev D, Timoshenko VY, Fujii M. Form birefringence of anisotropically nanostructured silicon. *Phys Rev B* 2005:71.
- [62] Diener J, Kunzner N, Gross E, Kovalev D, Fujii M. Silicon based optical devices – photonic applications of anisotropically nanostructured silicon. *Phys Status Solidi A* 2005;202:1432.
- [63] Ghulinyan M, Oton CJ, Gaburro Z, Pavesi L, Toninelli C, Wiersma DS. Zener tunneling of light waves in an optical superlattice. *Phys Rev Lett* 2005:94.
- [64] Applied Nanotech, Inc. (subsidiary of Nano-Proprietary, Inc.). Available from <http://www.nano-proprietary.com/index.htm?ani.htm>.
- [\*65] Saarinen JJ, Weiss SM, Fauchet PM, Sipe JE. Optical sensor based on resonant porous silicon structures. *Opt Express* 2005;13:3754.
- [66] Tsubaki K, Yamanaka H, Kitada K, Komoda T, Koshida N. Three-dimensional image sensing in air by thermally induced ultrasonic emitter based on nanocrystalline porous silicon. *Jpn J Appl Phys, Part 1* 2005;44:4436.
- [67] Archer M, Christophersen M, Fauchet PM. Electrical porous silicon chemical sensor for detection of organic solvents. *Sens Actuators B* 2005;106:347.
- [68] Archer M, Christophersen M, Fauchet PM. Macroporous silicon electrical sensor for DNA hybridization detection. *Biomed Microdevices* 2004;6:203.
- [69] Steinem C, Janshoff A, Lin V S-Y, Völcker NH, Ghadiri MR. DNA hybridization-enhanced porous silicon corrosion: mechanistic investigations and prospect for optical interferometric biosensing. *Tetrahedron* 2004;60:11259.
- [70] Kalkan AK, Henry MR, Li H, Cuiffi JD, Hayes DJ, Palmer C, et al. Biomedical/analytical applications of deposited nanostructured Si films. *Nanotechnology* 2005;16:1383.
- [71] Luongo K, Sine A, Bhansali S. Development of a highly sensitive porous Si-based hydrogen sensor using Pd nano-structures. *Sens Actuators B* 2005;111–112:125.
- [72] De Stefano L, Moretti L, Rendina I, Rotiroli L. Pesticides detection in water and humic solutions using porous silicon technology. *Sens Actuators B* 2005;111–112:522.
- [73] Lillis B, Jungk C, Iacopino D, Whelton A, Hurley E, Sheehan MM, et al. Microporous silicon and biosensor development: structural analysis, electrical characterisation and biocapacity evaluation. *Biosens Bioelectron* 2005;21:282.
- [74] Lewis SE, DeBoer JR, Gole JL, Hesketh PJ. Sensitive, selective, and analytical improvements to a porous silicon gas sensor. *Sens Actuators B* 2005;110:54.
- [75] Mathew FP, Alcolija EC. Porous silicon-based biosensor for pathogen detection. *Biosens Bioelectron* 2005;20:1656.
- [76] DeLouise LA, Fauchet PM, Miller BL, Pentland AA. Hydrogel-supported optical-microcavity sensors. *Adv Mater* 2005;17: 2199.
- [77] DeLouise LA, Kou PM, Miller BL. Cross-correlation of optical microcavity biosensor response with immobilized enzyme activity. Insights into biosensor sensitivity. *Anal Chem* 2005;77:3222.
- [78] DeLouise LA, Miller BL. Enzyme immobilization in porous silicon: quantitative analysis of the kinetic parameters for glutathione-S-transferases. *Anal Chem* 2005;77:1950.

- [79] DeLouise LA, Miller BL. Quantitative assessment of enzyme immobilization capacity in porous silicon. *Anal Chem* 2004;76:6915.
- [\*80] Pacholski C, Sartor M, Sailor MJ, Cunin F, Miskelly GM. Biosensing using porous silicon double-layer interferometers: reflective interferometric Fourier transform spectroscopy. *J Am Chem Soc* 2005;127:11636.
- [81] Afonso C, Budimir N, Fournier F, Tabet JC. Activated surfaces for laser desorption mass spectrometry: application for peptide and protein analysis. *Curr Pharm Design* 2005;11:2559.
- [82] Pihlainen K, Grigoros K, Franssila S, Ketola R, Kotiaho T, Kostianen R. Analysis of amphetamines and fentanyl by atmospheric pressure desorption/ionization on silicon mass spectrometry and matrix-assisted laser desorption/ionization mass spectrometry and its application to forensic analysis of drug seizures. *J Mass Spectrom* 2005;40:539.
- [83] Li Q, Ricardo A, Benner SA, Winefordner JD, Powell DH. Desorption/ionization on porous silicon mass spectrometry studies on pentose-borate complexes. *Anal Chem* 2005;77:4503.
- [84] Go EP, Apon JV, Luo G, Saghatelian A, Daniels RH, Sahi V, et al. Desorption/ionization on silicon nanowires. *Anal Chem* 2005;77:1641.
- [85] Gorecka-Drzazga A, Dziuban J, Drzazga W, Kraj A, Silberring J. Desorption/ionization mass spectrometry on array of silicon microtips. *J Vac Sci Technol B* 2005;23:819.
- [86] Yerokhov VY, Melnyk II. Porous silicon in solar cell structures: a review of achievements and modern directions of further use. *Renew Sustainable Energy Rev* 1999;3:291.
- [\*\*87] Sun W, Kherani NP, Hirschman KD, Gadenken LL, Fauchet PM. A three-dimensional porous silicon p-n diode for betavoltaics and photovoltaics. *Adv Mater* 2005;17:1230.
- [88] Striemer CC, Fauchet PM. Dynamic etching of silicon for solar cell applications. *Phys Status Solidi A* 2003;197:502.
- [89] Aouida S, Saadoun M, Boujmil MF, Ben Rabha M, Bessais B. Effect of UV irradiations on the structural and optical features of porous silicon: application in silicon solar cells. *Appl Surf Sci* 2004;238:193.
- [\*90] Peng K, Xu Y, Wu Y, Yan Y, Lee S-T, Zhu J. Aligned single-crystal Si nanowire arrays for photovoltaic applications. *Small* 2005;1:1062.
- [91] Tian L, Bhargava Ram K, Ahmad I, Menon L, Holtz M. Optical properties of a nanoporous array in silicon. *J Appl Phys* 2005;97:026101.
- [92] Hassen M, Ben Jaballah A, Hajji M, Khedher N, Bessais B, Ezzaouia H, et al. Performance improvements of crystalline silicon by iterative gettering process for short duration and with the use of porous silicon as sacrificial layer. *Sol Energy Mater* 2005;87:493.
- [93] Khedher N, Hajji M, Hassen M, Ben Jaballah A, Ouertani B, Ezzaouia H, et al. Gettering impurities from crystalline silicon by phosphorus diffusion using a porous silicon layer. *Sol Energy Mater* 2005;87:605.
- [94] Hajji M, Ben Jaballah A, Hassen M, Khedher N, Rahmouni H, Bessais B, et al. Silicon gettering: some novel strategies for performance improvements of silicon solar cells. *J Mater Sci* 2005;40:1419.
- [95] Khedher N, Ben Jaballah A, Hassen M, Hajji M, Ezzaouia H, Bessais B, et al. Gettering by heat thermal processing: application in crystalline silicon solar cells. *Mater Sci Semicond Process* 2004;7:439.
- [96] Solanki CS, Carnel L, Van Nieuwenhuysen K, Ulyashin A, Posthuma N, Beaucarne G, et al. Thin-film free-standing monocrystalline Si solar cells with heterojunction emitter. *Prog Photovoltaics* 2005;13:201.
- [\*\*97] Duerinckx F., Van Nieuwenhuysen K, Kim HJ, Kuzma-Filipek I, Beaucarne G, Poortmans J. Light trapping for epitaxial thin film crystalline silicon solar cells. In: *Proc 20th Euro Photovoltaic Solar Energy Conf*, 2005. p. 1190.
- [98] Aricò AS, Bruce P, Scrosati B, Tarascon JM, Van Schalkwijk W. Nanostructured materials for advanced energy conversion and storage devices. *Nature Mater* 2005;4:366.
- [\*99] Shin HC, Corno JA, Gole JL, Liu ML. Porous silicon negative electrodes for rechargeable lithium batteries. *J Power Sources* 2005;139:314.
- [100] Yamazaki Y. Application of MEMS technology to micro fuel cells. *Electrochim Acta* 2005;50:663.
- [101] Aravamudhan S, Rahman ARA, Bhansali S. Porous silicon based orientation independent, self-priming micro direct ethanol fuel cell. *Sens Actuators A* 2005;123–124:497.
- [\*102] Pichonat T, Gauthier-Manuel B. Development of porous silicon-based miniature fuel cells. *J Micromech Microeng* 2005;15: S179.
- [103] Foraker AB, Walczak RJ, Cohen MH, Boiarski TA, Grove CF, Swaan PW. Biocompatible por-Si. *Pharm Res* 2003;20:110.
- [104] Canham LT. Bioactive silicon structure fabrication through nanoetching techniques. *Adv Mater* 1995;7:1033.
- [105] Canham LT. Derivatized mesoporous silicon with dramatically improved stability in simulated human blood plasma. *Adv Mater* 1999;11:1505.
- [106] Kim YH, Song H, Riu DH, Kim SR, Kim HJ, Moon JH. Preparation of porous Si-incorporated hydroxyapatite. *Curr Appl Phy* 2005;5:538.
- [107] Anglin EJ, Schwartz MP, Ng VP, Perelman LA, Sailor MJ. Engineering the chemistry and nanostructure of porous silicon Fabry-Perot films for loading and release of a steroid. *Langmuir* 2004;20:11264.
- [108] Salonen J, Paski J, Vaha-Heikkila K, Heikkila T, Bjorkqvist M, Lehto VP. Determination of drug load in porous silicon microparticles by calorimetry. *Phys Status Solidi A* 2005;202:1629.
- [109] Lehto VP, Vaha-Heikkila K, Paski J, Salonen J. Use of thermoanalytical methods in quantification of drug load in mesoporous silicon microparticles. *J Thermal Anal Calorimetry* 2005;80:393.
- [110] Robbins H, Schwartz B. Chemical etching of silicon. I. The system HF, HNO<sub>3</sub>, and H<sub>2</sub>O. *J Electrochem Soc* 1959;106:505.
- [111] Robbins H, Schwartz B. Chemical etching of silicon. II. The system HF, HNO<sub>3</sub>, H<sub>2</sub>O and HC<sub>2</sub>H<sub>3</sub>O<sub>2</sub>. *J Electrochem Soc* 1960;107:108.
- [112] Robbins H, Schwartz B. Chemical Etching of Silicon. III. A temperature study in the acid system. *J Electrochem Soc* 1961;108:365.
- [\*113] Turner DR. On the mechanism of chemically etching germanium and silicon. *J Electrochem Soc* 1960;107:810.
- [114] Uhler A. *Bell Syst Tech J* 1956;35:333.
- [115] Sarathy J, Shih S, Jung K, Tsai C, Li K-H, Kwong D-L, et al. Demonstration of photoluminescence in nonanodized silicon. *Appl Phys Lett* 1992;60:1532.
- [116] Fathauer RW, George T, Ksendzov A, Vasquez RP. Visible luminescence from silicon wafers subjected to stain etches. *Appl Phys Lett* 1992;60:995.
- [117] Steckl AJ, Xu J, Mogul HC. Crystallinity and photoluminescence in stain-etched porous Si. *J Electrochem Soc* 1994;141:674.
- [118] Beale MIJ, Benjamin JD, Uren MU, Chew NG, Cullis AG. The formation of porous silicon by chemical stain etches. *J Cryst Growth* 1986;75:408.
- [119] Schoisswohl M, Cantin JL, von Bardeleben HJ, Amato G. Electron paramagnetic resonance study of luminescent stain etched porous silicon. *Appl Phys Lett* 1995;66:3660.
- [120] Rappich J, Lewerenz HJ. Photo- and potential-controlled nanoporous silicon formation on n-Si(111): An in situ FTIR investigation. *Thin Solid Films* 1996;276:25.
- [121] Gerischer H, Lübke M. Electrolytic growth and dissolution of oxide layers on silicon in aqueous solutions of fluorides. *Ber Bunsen-Ges Phys Chem* 1988;92:573.
- [122] Peiner E, Schlachetzki A. Anodic dissolution during electrochemical carrier-concentration profiling of silicon. *J Electrochem Soc* 1992;139:552.

- [123] Smith RL, Collins SD. Porous silicon formation mechanisms. *J Appl Phys* 1992;71:R1.
- [\*124] Kooij ES, Vanmaekelbergh D. Catalysis and pore initiation in the anodic dissolution of silicon in HF. *J Electrochem Soc* 1997;144:1296.
- [\*125] Gerischer H, Allongue P, Costa Kieling V. The mechanism of the anodic oxidation of silicon in acidic fluoride solutions revisited. *Ber Bunsen-Ges Phys Chem* 1993;97:753.
- [126] Allongue P, Kieling V, Gerischer H. Etching mechanism and atomic structure of H-Si(111) surfaces prepared in NH<sub>4</sub>F. *Electrochim Acta* 1995;40:1353.
- [127] Kang Y, Jorné J. Photoelectrochemical dissolution of n-type silicon. *Electrochim Acta* 1998;43:2398.
- [\*128] Lehmann V, Gösele U. Porous silicon formation: a quantum wire effect. *Appl Phys Lett* 1991;58:856.
- [129] Koker L, Kolasinski KW. Laser-assisted formation of porous silicon in diverse fluoride solutions: reactions kinetics and mechanistic implications. *J Phys Chem B* 2001;105:3864.
- [130] Zaroni R, Righini G, Mattogno G, Schirone L, Sotgiu G, Rallo F. X-ray photoelectron spectroscopy characterization of stain-etched luminescent porous silicon films. *J Lumin* 1998;80:159.
- [131] Kelly MT, Chun JKM, Bocarsly AB. High efficiency chemical etchant for the formation of luminescent porous silicon. *Appl Phys Lett* 1994;64:1693.
- [132] Judge JS. A study of the dissolution of SiO<sub>2</sub> in acidic fluoride solutions. *J Electrochem Soc* 1971;118:1772.
- [133] Somashekhar A, O'Brien S. Etching SiO<sub>2</sub> films in aqueous 0.49% HF. *J Electrochem Soc* 1996;143:2885.
- [134] Osseo-Asare K. Etching kinetics of silicon dioxide in aqueous fluoride solutions: a surface complexation model. *J Electrochem Soc* 1996;143:1339.
- [135] Frohnhoff S, Marso M, Berger MG, Thönissen M, Lüth H, Münder H. An extended quantum model for porous silicon formation. *J Electrochem Soc* 1995;142:615.
- [136] van Buuren T, Dinh LN, Chase LL, Siekhaus WJ, Terminello LJ. Changes in the electronic properties of Si nanocrystals as a function of particle size. *Phys Rev Lett* 1998;80:3803.
- [137] Velasco JG. Open-circuit study of stain etching processes leading to the formation of porous silicon layers. *J Electrochem Soc* 2003;150:C335.
- [\*\*138] Nahidi M, Kolasinski KW. The effects of stain etchant composition on the photoluminescence and morphology of porous silicon. *J Electrochem Soc* 2006;153:C19.
- [139] Dimova-Malinovska D, Sendova-Vassileva M, Tzenov N, Kamenova M. Preparation of thin porous silicon layers by stain etching. *Thin Solid Films* 1997;297:9.
- [140] Ashruf CMA, French PJ, Bressers PMMC, Kelly JJ. Galvanic porous silicon formation without external contacts. *Sens Actuators A* 1999;74:118.
- [141] Xia XH, Ashruf CMA, French PJ, Kelly JJ. Galvanic cell formation in silicon/metal contacts: the effect on silicon surface morphology. *Chem Mater* 2000;12:1671.
- [\*142] Li X, Bohn PW. Metal-assisted chemical etching in HF/H<sub>2</sub>O<sub>2</sub> produces porous silicon. *Appl Phys Lett* 2000;77:2572.
- [143] Harada Y, Li X, Bohn PW, Nuzzo RG. Catalytic amplification of the soft lithographic patterning of Si. Nonelectrochemical orthogonal fabrication of photoluminescent porous Si pixel arrays. *J Am Chem Soc* 2001;123:8709.
- [144] Chattopadhyay S, Li X, Bohn PW. In-plane control of morphology and tunable photoluminescence in porous silicon produced by metal-assisted electroless chemical etching. *J Appl Phys* 2002;91:6134.
- [145] Chattopadhyay S, Bohn PW. Direct-write patterning of microstructured porous silicon arrays by focused-ion-beam Pt deposition and metal-assisted electroless etching. *J Appl Phys* 2004;96:6888.
- [146] Yae S, Kawamoto Y, Tanaka H, Fukumuro N, Matsuda H. Formation of porous silicon by metal particle enhanced chemical etching in HF solution and its application for efficient solar cells. *Electrochem Commun* 2003;5:632.
- [147] Gorostiza P, Diaz R, Kulandainathan MA, Sanz F, Morante JR. Simultaneous platinum deposition and formation of a photoluminescent porous silicon layer. *J Electroanal Chem* 1999;469:48.
- [148] Gorostiza P, Anbu Kulandainathan M, Diaz R, Sanz F, Allongue P, Morante JR. Charge exchange processes during the open-circuit deposition of nickel on silicon from fluoride solutions. *J Electrochem Soc* 2000;147:1026.
- [\*149] Gorostiza P, Allongue P, Diaz R, Morante JR, Sanz F. Electrochemical Characterization of the open-circuit deposition of platinum on silicon from fluoride solutions. *J Phys Chem B* 2003;107:6454.
- [150] Hadjersi T, Gabouze N, Ababou A, Boumaour M, Chergui W, Cheraga H, et al. Metal-assisted chemical etching of multicrystalline silicon in HF/Na<sub>2</sub>S<sub>2</sub>O<sub>8</sub> produces porous silicon. *Mater Sci Forum* 2005;480–481:139.
- [151] Mitsugi N, Nagai K. Pit formation induced by copper contamination on silicon surface immersed in dilute hydrofluoric acid solution. *J Electrochem Soc* 2004;151:G302.
- [152] Peng K, Yan Y, Gao S, Zhu J. Dendrite-assisted growth of silicon nanowires in electroless metal deposition. *Adv Func Mater* 2003;13:127.
- [153] Peng K-Q, Yan Y-J, Gao S-P, Zhu J. Synthesis of large-area silicon nanowire arrays via self-assembling nanoelectrochemistry. *Adv Mater* 2002;14:1164.
- [154] Peng KQ, Huang ZP, Zhu J. Fabrication of large-area silicon nanowire p-n junction diode arrays. *Adv Mater* 2004;16:73.
- [\*\*155] Peng KQ, Wu Y, Fang H, Zhong XY, Xu Y, Zhu J. Uniform, axial-orientation alignment of one-dimensional single-crystal silicon nanostructure arrays. *Angew Chem, Int Ed Engl* 2005;44: 2737.
- [156] Tsujino K, Matsumura M. Helical nanoholes bored in silicon by wet chemical etching using platinum nanoparticles as catalyst. *Electrochem Solid State Lett* 2005;8:C193.
- [157] Tsujino K, Matsumura M. Boring deep cylindrical nanoholes in silicon using silver nanoparticles as a catalyst. *Adv Mater* 2005;17:1045.
- [158] Cruz S, Hönig-d'Orville A, Müller J. Fabrication and optimization of porous silicon substrates for diffusion membrane applications. *J Electrochem Soc* 2005;152:C418.
- [159] Ben Rabha M, Saadoun M, Boujmil MF, Bessaïs B, Ezzaouia H, Bennaceur R. Application of the chemical vapor-etching in polycrystalline silicon solar cells. *Appl Surf Sci* 2005;252:488.
- [160] Ben Jaballah A, Hassen M, Hajji M, Saadoun M, Bessaïs B, Ezzaouia H. Chemical vapour etching of silicon and porous silicon: silicon solar cells and micromachining applications. *Phys Status Solidi A* 2005;202:1606.
- [161] Ben Jaballah A, Saadoun M, Hajji A, Ezzaouia H, Bessaïs B. Silicon dissolution regimes from chemical vapour etching: from porous structures to silicon grooving. *Appl Surf Sci* 2004;238:199.
- [162] Saadoun M, Bessaïs B, Mliki N, Ferid M, Ezzaouia H, Bennaceur R. Formation of luminescent (NH<sub>4</sub>)<sub>2</sub>SiF<sub>6</sub> phase from vapour etching-based porous silicon. *Appl Surf Sci* 2003;210:240.
- [163] Saadoun M, Mliki N, Kaabi H, Daoudi K, Bessaïs B, Ezzaouia H, et al. Vapour-etching-based porous silicon: a new approach. *Thin Solid Films* 2002;405:29.
- [164] Koker L, Wellner A, Sherratt PAJ, Neuendorf R, Kolasinski KW. Laser-assisted formation of porous silicon in diverse fluoride solutions: Hexafluorosilicate deposition. *J Phys Chem B* 2002;106:4424.
- [165] Mills D, Kolasinski KW. Laser-etched silicon pillars and their porosification. *J Vac Sci Technol, A* 2004;22:1647.
- [166] Mills D, Nahidi M, Kolasinski KW. Stain etching of silicon pillars and macropores. *Phys Status Solidi A* 2005;202:1422–6.